

# Fractal atom-photon dynamics in a cavity

*To the memory of my beloved daughter Maria*

S.V. Prants

*Laboratory of Nonlinear Dynamical Systems, V.I.Il'ichev Pacific Oceanological  
Institute of the Russian Academy of Sciences, 690041 Vladivostok, Russia*

Nonlinear dynamics in the fundamental interaction between a two-level atom with recoil and a quantized radiation field in a high-quality cavity is studied. We consider the strongly coupled atom-field system as a quantum-classical hybrid with dynamically coupled quantum and classical degrees of freedom. We show that, even in the absence of any other interaction with environment, the interaction of the purely quantum atom-field system with the external atomic degree of freedom provides the emergence of classical dynamical chaos from quantum electrodynamics. Atomic fractals with self-similar intermittency of smooth and unresolved structures are found in the exit-time scattering function. Tiny interplay between all the degrees of freedom is responsible for dynamical trapping of atoms even in a very short microcavity. Gedanken experiments are proposed to detect manifestations of atomic fractals in cavity quantum electrodynamics.

PACS numbers: 42.50.Vk, 05.45.Df

## I. INTRODUCTION

The emergence of classical dynamical chaos from more profound quantum mechanics is one of the most intriguing problems in physics [1, 2, 3, 4]. Dynamical chaos in classical mechanics is a special kind of random motion in dynamical systems without any noise and random parameters that is characterized by sensitive dependence on initial conditions in a bounded phase space. The current consensus is that *isolated bounded quantum systems* do not show sensitive dependence on initial conditions in the same way as classical systems because their evolution is unitary. So the question is: What is the fundamental mechanism of arising classical chaos from quantum mechanics?

The purpose of this lecture is to show how classical Hamiltonian chaos with sensitive dependence on initial conditions, positive Lyapunov exponents, fractal properties of underlying phase space, and anomalous statistical characteristics may arise from quantum electrodynamics of a single atom strongly interacting with a quantized mode of the electromagnetic radiation field in a high-quality cavity. The study of the fundamental atom-photon interaction constitutes the rapidly growing field of cavity quantum electrodynamics (for a review see [5, 6, 7, 8]). The experimental state of the art has reached in this field the stage where the transition from classical to quantum dynamical regimes can now be probed directly. Atoms and photons, confined in a high-quality cavity, are ideal objects to study quantum-classical correspondence and quantum chaos.

Real quantum systems are not isolated. They interact with their environment and in attempts to measure their states with classical measuring devices which should, by virtue of their purpose, be in unstable states. So we are dealing with quantum-classical hybrids. It is not a simple question which degrees of freedom should be considered in a given physical

situation as quantum ones and which ones as classical. Let us consider an excited atom in a single-mode high-quality cavity whose frequency is close to the frequency of one of the atomic electro-dipole transitions. The atom emits a photon in the cavity mode and goes to a lower-lying state. Under the conditions of the strong atom-field coupling, the photon may be reemitted and reabsorbed by the atom many times. Sooner or later, the atom will emit a photon in one of the other modes of the electromagnetic field that are not sustained by the cavity (for example, transverse modes in an open Fabry-Perot cavity) and the photon will be lost in a surrounding, the process known as spontaneous emission. In real experiments, the cavity relaxation due to the losses in the cavity walls cannot be neglected. It is usually modeled by a weak coupling of the selected cavity mode with a bath of harmonic oscillators (spanning a wide frequency range) in thermal equilibrium at a given temperature. Sooner or later, the atom will relax to a lower-lying state that is not resonant with the cavity mode. It seems to be reasonable to treat two near-resonant atomic levels, strongly coupled to a cavity mode, as a quantum dynamical system weakly coupled to the other electromagnetic modes, the other atomic levels and the cavity walls. An infinite number of the respective degrees of freedom, which are coupled to the quantum dynamical system's degrees of freedom but are not affected by them, forms an inexhaustible external reservoir (that may be treated classically) usually called "the environment". It is a kind of the external coupling which is inevitably present in reality.

There is another kind of coupling called the dynamical coupling. For example, if the average number of photons in the cavity mode is sufficiently large, one may treat the field as a classical object dynamically coupled to quantized atoms (the semiclassical approximation) and take into account the feedback effect of the atoms on the radiation field. The semiclassical approximation breaks down when we deal with sin-

gle cold atoms and photons in a cavity. In this situation we should take into account the translational (external) atomic degree of freedom. When a cold atom emits and absorbs photons its momentum and position may vary significantly due to the recoil effect. The external atomic degree of freedom, which may be treated classically if the values of the atomic momentum are greater than the photon momentum, is dynamically coupled to the internal atomic and field degrees of freedom which are treated quantum mechanically. We show in this lecture that, even in the absence of any other interaction with the environment, the interaction of the quantum atom-field system with the external atomic degree of freedom provides, under appropriate conditions, the emergence of classical chaos from quantum electrodynamics.

## II. EARLY STUDIES OF CLASSICAL CHAOS IN THE ATOM-FIELD INTERACTION

The discovery that a single-mode laser, a symbol of coherence and stability, may exhibit deterministic chaos is especially important not only because lasers are one of the main instruments in physics but lasers, as well, provide almost ideal systems to test general ideas in quantum mechanics and statistical physics. From the standpoint of nonlinear dynamics, laser is an open dissipative system that transforms an external excitation into a coherent output in the presence of loss. Some manifestations of strange attractors and dissipative chaos have been observed with different types of lasers (for a review, see [9, 10, 11]). A collection of identical two-level atoms, interacting with a single-mode electromagnetic field, provides the simplest model for laser dynamics. Because of a large number of atoms (and photons), laser dynamics can be adequately described in the so-called semiclassical approximation, where one treats atoms as two-level objects, which may be described by the Bloch equations for two components of the collective electro-dipole polarisation and collective atomic population inversion, interacting with a field mode to be governed by the classical Maxwell equations for the field strengths with the right hands depending on the atomic polarisation. With a single-mode homogeneously broadened laser, operating in resonance with the gain center, these five equations can be reduced to three real-valued equations for slowly varying amplitudes which have been shown to be equivalent to the well-known Lorenz model for fluid convection [12].

Practically in the same time, ideas of dynamical chaos have been explored with fundamental models of the matter-radiation interaction, comprising of a collection of two-level atoms *interacting with their own radiation field* in a perfect single-mode cavity without any loss and external excitation. It has been shown theoretically and numerically [13] that the semiclassical Maxwell-Bloch equations, following

from the Dicke Hamiltonian [14], may demonstrate *Hamiltonian semiclassical chaos* if one goes beyond the so-called rotating-wave approximation, i. e. if one takes into account energy non-conserving terms in the Hamiltonian (for details, see the beginning of the next section). This mechanism of arising Hamiltonian semiclassical chaos is rather weak under realistic assumptions. On the other hand, rotating-wave approximation suppresses chaos with atoms at rest due to existence of an additional integral of motion, the conserving interaction energy. It has been shown in a series of our papers [15, 16, 17, 18, 19] that Hamiltonian chaos may arise within the rotating-wave approximation under conditions of a modulation of the atom-field interaction. In a natural way it occurs when atoms move through a cavity in a direction along which the cavity sustains a standing-wave field that is periodic in space [16, 18]. When moving with a constant velocity, atoms “see” the field whose strength changes in time periodically. It breaks down the interaction-energy integral and may cause Hamiltonian semiclassical chaos of a homoclinic type [16, 18, 19]. There are another ways of modulations to be considered in [17, 20]. The modulation of the detuning between the atomic transition frequency and the frequency of the field mode has been shown to produce parametric instability and Hamiltonian semiclassical chaos [17]. Structural Hamiltonian chaos [20] may arise as a result of a harmonic modulation of cavity length which causes the respective oscillations of the nodes of a standing-wave.

Generally speaking, the model of the atom-field interaction should involve not only the internal atomic and field degrees of freedom but also the center-of-mass motion of the atom. When emitting and absorbing photons, atoms not only change their internal states but their position and momentum are changed as well due the photon recoil effect. This effect may be neglected if one deals with Rydberg atoms interacting with a microwave field in a cavity (as it has been done in [15, 16, 18, 19, 20]) or with thermal usual atoms interacting with a visible light. It has been theoretically and numerically shown in [21, 22] that Hamiltonian semiclassical chaos may arise with cold atoms with recoil in a standing-wave microcavity.

In trying to describe adequately dynamics of single atoms and photons in a high-quality cavity, one should go beyond the semiclassical approximation and treats the atom-photon interaction on a quantum ground. The fully quantum model of the interaction between a single two-level atom (without a recoil) with a single-mode quantized field in an ideal cavity is known as the Jaynes-Cummings model [23]. It describes the atom-field system as a quantum-electrodynamical object whose evolution in time is (quasi)periodic. In Schrödinger picture, it may be described by an infinite set of linear ordinary differential equations for the probability amplitudes to find the atom in the ground/excited state and the field in the state with

$n$  photons, where  $n$  runs from zero to infinity. When adopting the semiclassical approximation, we reduce, by hook or by crook, this infinite set to a small number of equations for atomic and field variables. In fact, we decouple the quantum atom-field system into an atom and field parts which may exchange excitations with each other. In doing so, we get automatically products of the atom and field variables in the equations of motion. The respective Maxwell–Bloch equations may, under appropriate conditions, produce chaos in the classical sense of sensitive dependence on initial conditions in the reduced classical phase space spanned by the atomic and field expectation values. It resembles the procedure of deriving the famous Lorenz equations from an infinite hierarchy of mode equations in fluid convection by reducing it to three main modes only.

The reduction of an infinite set of linear equations, that are not chaotic in the classical sense, to a finite set of nonlinear equations, that may be chaotic, makes an impression that it is only a mathematical trick. It seems that it is not only a useful trick enabling us to handle with the equations of motion but the reduction is a model of processes that may occur in nature. Coherence loss caused by inevitable interaction with environment (decoherence) breaks quantum unitarity suppressing some quantum properties of motion and revealing its classical properties. Such a situation can be modeled with the use of a quantum-classical hybrid, a system with quantum and classical degrees of freedom dynamically coupled to each other. Which part of the whole system under consideration is quantized and which one is treated classically depends on the physical situation. If we have a large number of atoms (or photons) we may adopt with a good accuracy the semiclassical approximation treating the cavity field as a classical one. When considering a single atom with a recoil in a high-quality microcavity it is necessary to quantize the internal electronic atomic and field degrees of freedom but the translational atomic motion may be treated classically if the values of the atomic momentum are greater than the photon momentum.

### III. ATOM WITHOUT RECOIL INTERACTING WITH A QUANTIZED RADIATION FIELD IN AN IDEAL CAVITY

The interaction between matter and radiation, commonly evidenced by spontaneous emission and induced emission and absorption of photons by atoms, is one of the most fundamental dynamical interactions in nature. In free space, an excited atomic state decays irreversibly because an infinity of vacuum electromagnetic states is available to the radiated photons which disappears in the free-space mode continuum. The situation may be changes if the mode structure and the density of modes are modified by placing the radiating

atom into a high-quality cavity. A cavity-induced enhancement and inhibition of spontaneous emission has been observed in a number of experiments in different ranges of the electromagnetic field, from microwaves to visible light (for a review see [6, 24]).

In a near-resonant ideal cavity with a single-mode frequency closed to the atomic transitional frequency, the radiation emitted by the atom is reflected at the cavity walls and is reabsorbed by the atom many times before it dissipates. In particularly, spontaneous emission becomes reversible. In cavity quantum electrodynamics near-resonant interaction of a single atom with a single-mode cavity field is commonly modeled by the Hamiltonian

$$\hat{H} = \hat{H}_a + \hat{H}_f + \hat{H}_{int}, \quad (1)$$

where

$$\hat{H}_a = \frac{1}{2}\hbar\omega_a\hat{\sigma}_z \quad (2)$$

represents the free motionless two-level atom with  $\hbar\omega_a$  being the energy separation between the electronic states, the ground  $|1\rangle$  and excited  $|2\rangle$  ones. The Pauli spin operator acts on the states as

$$\hat{\sigma}_z|1\rangle = -|1\rangle, \quad \hat{\sigma}_z|2\rangle = |2\rangle. \quad (3)$$

The Hamiltonian

$$\hat{H}_f = \hbar\omega_f(\hat{a}^\dagger\hat{a} + \frac{1}{2}) \quad (4)$$

represents the mode of the isolated field. The photon annihilation  $\hat{a}$  and creation  $\hat{a}^\dagger$  operators with the commutation rule  $[\hat{a}, \hat{a}^\dagger] = 1$  act on the photon number states as follows:

$$\hat{a}|n\rangle = \sqrt{n}|n-1\rangle, \quad \hat{a}^\dagger|n\rangle = \sqrt{n+1}|n+1\rangle. \quad (5)$$

The electric dipole interaction between the atom and the field mode is described by the operator

$$\hat{H}_{int} = \hbar\Omega_0(x)(\hat{a} + \hat{a}^\dagger)(\hat{\sigma}_+ + \hat{\sigma}_-) \simeq \hbar\Omega_0(x)(\hat{a}\hat{\sigma}_+ + \hat{a}^\dagger\hat{\sigma}_-), \quad (6)$$

where  $\Omega_0(x)$  is the atom-field coupling constant at the atomic position  $x$  in the one-dimensional cavity, which is known under the names “vacuum or single-photon Rabi frequency”. The Pauli spin operators  $\hat{\sigma}_\pm$  with the commutation rules  $[\hat{\sigma}_\pm, \hat{\sigma}_z] = \mp 2\hat{\sigma}_\pm$ ,  $[\hat{\sigma}_+, \hat{\sigma}_-] = \hat{\sigma}_z$  describe transitions between the ground and excited electronic states

$$\hat{\sigma}_+|1\rangle = |2\rangle, \quad \hat{\sigma}_-|2\rangle = |1\rangle, \quad \hat{\sigma}_+|2\rangle = \hat{\sigma}_-|1\rangle = 0. \quad (7)$$

The first form of the Hamiltonian (6) follows from the quantization of the classical electric dipole atom-field interaction by replacing the atomic dipole moment by the operator  $\hat{\sigma}_x = \hat{\sigma}_+ + \hat{\sigma}_-$  and the classical electric field by the operator  $\hat{a} + \hat{a}^\dagger$ . The products

$\hat{a}^\dagger\hat{\sigma}_-$  and  $\hat{a}\hat{\sigma}_+$  describe the transition of the atom from the ground (excited) to the excited (ground) state and simultaneous annihilating (creating) a photon in the field mode, respectively. They are usual energy-conserving processes. The product  $\hat{a}^\dagger\hat{\sigma}_+$  describes the transition of the atom from the ground to the excited state and simultaneous creating a photon in the mode. The reverse process of simultaneous atom and field de-excitation is described by the term  $\hat{a}\hat{\sigma}_-$ . The last two processes are not energy-conserving and may be neglected while we deal with a single atom. Omitting the energy-nonconserving terms defines the Jaynes-Cummings model [23] which was proposed originally in 1963 as a purely theoretical tool for studying fundamentals of the interaction between matter and radiation. It seemed to be far from reality because neither the atom nor the cavity mode can hardly be perfectly isolated from environment with those-days technique. Exciting progress in experimental techniques has drastically changed the situation. Experiments, using very high-quality microwave cavities with  $Q \sim 10^{10}$  and optical microcavities with  $Q \sim 10^6$ , have now achieved the exceptional circumstance of strong coupling between atoms and a cavity field with the strength of the coupling exceeding the atomic and cavity decays that provides manipulations with single atoms and photons and experimental proving of some predictions of the Jaynes-Cummings model [5, 6, 7, 8]. The art of experimentalists and theoretical efforts have opened exciting perspectives for realizing gedanken experiments on fundamentals of quantum mechanics and implementing quantum communications and computing. As we will show in this lecture, an atom, interacting with a radiation field in a high- $Q$  cavity, provides an example of strongly-coupled microscopic nonlinear system whose dynamics may be very complicated and even chaotic.

The Jaynes-Cummings Hamiltonian has the form

$$\hat{H}_{JC} = \frac{1}{2}\hbar\omega_a\hat{\sigma}_z + \hbar\omega_f(\hat{a}^\dagger\hat{a} + \frac{1}{2}) + \hbar\Omega_0 f(x)(\hat{a}^\dagger\hat{\sigma}_- + \hat{a}\hat{\sigma}_+), \quad (8)$$

where  $\Omega_0$  is an amplitude value of the vacuum Rabi frequency and  $f(x)$  is a shape function of the cavity mode. Let us expand the atom-field state vector over the electronic atomic states and Fock (or photon-number) field states  $|n\rangle$

$$|\Psi(t)\rangle = \sum_{n=0}^{\infty} a_n(t) |2, n\rangle + b_n(t) |1, n\rangle, \quad (9)$$

where  $a_n(b_n)$  are probability amplitudes to find the atom in the excited (ground) state and  $n$  photons in the field mode, respectively. Substitution of Eqs.(8) and (9) into the Schrödinger equation

$$i\hbar\frac{d|\Psi(t)\rangle}{dt} = \hat{H}_{JC}|\Psi(t)\rangle \quad (10)$$

results in an infinite-dimensional set of coupled linear equations for the complex-valued probability amplitudes

$$\begin{aligned} \dot{a}_n &= -i [\Delta_a a_n + \sqrt{n+1} f(x) b_{n+1}], \\ \dot{b}_{n+1} &= i [\Delta_b b_{n+1}^* + \sqrt{n+1} f(x) a_n^*], \end{aligned} \quad (11)$$

where dot denotes differentiation with respect to dimensionless time  $\tau = \Omega_0 t$ ,  $\Delta_a = (n\omega_f + \omega_a/2)/\Omega_0$ , and  $\Delta_b = [(n+1)\omega_f - \omega_a/2]/\Omega_0$ . It is convenient to define new real-valued combinations of the probability amplitudes

$$\begin{aligned} u_n &= 2\text{Re}(a_n b_{n+1}^*), & v_n &= -2\text{Im}(a_n b_{n+1}^*), \\ z_n &= |a_n|^2 - |b_{n+1}|^2, \end{aligned} \quad (12)$$

for which we get from (11) the quantum Bloch-like equations of motion

$$\begin{aligned} \dot{u}_n &= \delta v_n, \\ \dot{v}_n &= -\delta u_n - 2\sqrt{n+1} f(x) z_n, \\ \dot{z}_n &= 2\sqrt{n+1} f(x) v_n, \quad n = 0, 1, 2, \dots, \end{aligned} \quad (13)$$

where  $\delta = (\omega_a - \omega_f)/\Omega_0$  is the dimensionless detuning between the atomic transition,  $\omega_a$ , and the field-mode,  $\omega_f$ , frequencies. For each specified photon number  $n$ , the quantity  $R_n^2 = u_n^2 + v_n^2 + z_n^2$  is conserved. Two global integrals of motion

$$\begin{aligned} W_{JC} &= \sum_{n=0}^{\infty} \sqrt{n+1} f(x) u_n - \frac{\delta}{2} \sum_{n=0}^{\infty} z_n, \\ \sum_{n=0}^{\infty} R_n &= 1 \end{aligned} \quad (14)$$

reflect conservation of the total energy and of the total probability, respectively. Eqs.(13) can be easily solved for each  $n$  in terms of trigonometric functions (we assume that  $f(x)$  does not depend on time). The general solution of the Schrödinger equation is the sum of the solutions of an infinite set of the independent Bloch-like equations. The exact general solution for one of the measured quantities, the atomic population inversion

$$z(\tau) = \sum_{n=0}^{\infty} z_n(\tau), \quad (15)$$

is the following:

$$\begin{aligned} z(\tau) &= \sum_{n=0}^{\infty} u_n(0) \frac{2\delta\sqrt{n+1} f(x)}{\Omega_n^2} (1 - \cos \Omega_n \tau) + \\ &v_n(0) \frac{2\sqrt{n+1} f(x)}{\Omega_n} \sin \Omega_n \tau + \\ &z_n(0) \frac{\delta^2 + 4(n+1) f^2(x) \cos \Omega_n \tau}{\Omega_n^2}, \end{aligned} \quad (16)$$

where

$$\Omega_n = \sqrt{\delta^2 + 4(n+1)f^2(x)} \quad (17)$$

is the  $n$ -photon Rabi frequency,  $u_n(0)$ ,  $v_n(0)$  and  $z_n(0)$  are the respective initial values which are determined by the initial atomic and field states. As it is seen from (16), the solution with initially sharply defined atomic and field energy states ( $|1\rangle$  or  $|2\rangle$  and  $|n\rangle$ ) describes a periodic exchange of one quantum of energy between the atom and the field.

The Fock state  $|n\rangle$  with a specified number of photons in the mode is an exotic field state. In general, a pure quantized field state is an infinite superposition of the photon-number states

$$|f\rangle = \sum_{n=0}^{\infty} c_n |n\rangle, \quad (18)$$

where  $p_n = |c_n|^2$  is the probability for observing  $n$  photons. The most classical of single-mode quantum states is a coherent state

$$|\alpha\rangle = e^{-|\alpha|^2/2} \sum_{n=0}^{\infty} \frac{\alpha^n}{n!} |n\rangle \equiv \sum_{n=0}^{\infty} c_n(\alpha) |n\rangle, \quad (19)$$

whose photon probabilities follow a Poisson distribution with the mean number of photons  $\langle n \rangle = |\alpha|^2$  and the root mean square spread  $\Delta n = |\alpha|$ . Evolution of the population inversion of an atom,  $z$ , in the field, initially prepared to be in a coherent state, contains all the Rabi frequencies  $\Omega_n$ . The incommensurability of Rabi frequencies for different  $n$  inevitably washes out the periodicity of population transfer resulting in a collapse of the excited-state occupation probability. Since the frequencies  $\Omega_n$  form a discrete set, the signal reappears after a time (see Fig. 1a computed with  $f(x) = 1$ ,  $\delta = 0$  and with the initial conditions (35)). The collapse-revival phenomenon, a direct demonstration of quantum nature of the radiation field, has been demonstrated experimentally [6, 25].

Let us consider as well another pure field state

$$|\chi\rangle = \sum_{n=0}^{\infty} c_n(\chi) |n\rangle, \quad (20)$$

whose photon probabilities follow a Bose-Einstein distribution

$$p_n(\chi) = \frac{\langle n \rangle^n}{(1 + \langle n \rangle)^{n+1}}. \quad (21)$$

Collapses and revivals also occur with this field state (see Fig. 1b computed with  $f(x) = 1$ ,  $\delta = 0$  and with the initial conditions (36)), but the collapse time is much shorter as compared with a coherent state because the Bose-Einstein spread in the photon number is far larger than for a coherent field with the same mean number of photons.

Fig. 1 demonstrates that the simple Jaynes-Cummings model with  $f(x) = 1$  may produce very

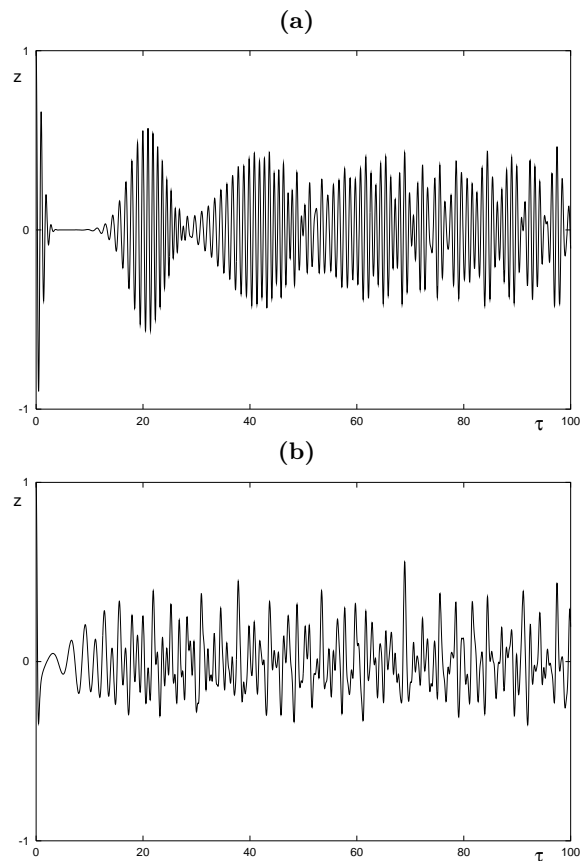


FIG. 1: Atomic population inversion  $z(\tau)$  for the resonant Jaynes-Cummings model with an initially excited motionless atom and (a) coherent and (b) Bose-Einstein initial states of the cavity quantized field.

complicated time evolution. However, the respective oscillations, of course, are not chaotic in the classical sense of exponential sensitivity to small changes in initial conditions. It is clear from the very structure of the equations of motion (13) which are infinite-dimensional but linear. In classical mechanics the phase space is continuous and states of a classical system can be arbitrarily close to each other providing a possibility of exponential diverging of initially close trajectories in a bounded region of the phase space. In quantum mechanics there is no notion of a trajectory, and the quantum phase space is not continuous due to the Heisenberg uncertainty principle. Evolution of an isolated quantum system is unitary and no dynamical chaos in the classical sense is possible with such systems. The notion "quantum chaos" just refers to the behavior of quantum systems whose classical counterparts behave chaotically [1, 2]. Real quantum systems are not isolated, they interact with their environment and, under attempts to measure their states, with classical devices which, by virtue of their purpose, should be in unstable states. Loosing of coherence, due to inevitable interaction with environment (decoherence), breaks down quantum unitarity

suppressing quantum properties of motion and manifesting classical ones. A quantum rotor with periodic kicks provides an illustrative example of suppressing quantum dynamical localization when one takes into account a thermal "bath" in the respective equations of motion [3]. In the next section we will elaborate these ideas with an extended version of the strongly coupled atom-field system considered above.

#### IV. A QUANTUM-CLASSICAL ATOM-FIELD HYBRID

In the process of emitting and absorbing photons of the cavity-field mode, the atom not only changes its internal electronic states but its external translational state is changed as well due to the photon recoil effect. In this section we consider a single two-level atom with mass  $m_a$  moving in an ideal cavity which sustains a single standing-wave mode along the axis  $x$  with the wave vector  $k_f$  and the shape function  $f(x) = -\cos(k_f \hat{x})$ . The respective Hamiltonian is the following extension of the Jaynes-Cummings Hamiltonian (8)

$$\hat{H} = \frac{1}{2m_a} \hat{p}^2 + \frac{1}{2} \hbar \omega_a \hat{\sigma}_z + \hbar \omega_f \hat{a}^\dagger \hat{a} - \hbar \Omega_0 (\hat{a}^\dagger \hat{\sigma}_- + \hat{a} \hat{\sigma}_+) \cos k_f \hat{x}, \quad (22)$$

where the momentum  $\hat{p}$  and position  $\hat{x}$  operators satisfy the standard commutation relation  $[\hat{x}, \hat{p}] = i\hbar$ . Operators, belonging to different degrees of freedom, commute with each other at the same time moment.

We have now three degrees of freedom, the internal atomic and the field ones, and the external (or translational) atomic degree of freedom. The first two degrees of freedom are treated as fully quantum ones in the Schrödinger picture. In fact, there are an infinite number of quantum degrees of freedom (see Eq. (13)) which are entangled. The external degree of freedom will be treated as the classical one that may be justified by large values of the atomic momentum as compared with the photon momentum  $\hbar k_f$ . The Hamilton equations of motion for the classical external degree of freedom is easily found from the Hamiltonian (22)

$$\frac{d \langle \hat{x} \rangle}{dt} = \frac{\partial \langle \hat{H} \rangle}{\partial \langle \hat{p} \rangle}, \quad \frac{d \langle \hat{p} \rangle}{dt} = -\frac{\partial \langle \hat{H} \rangle}{\partial \langle \hat{x} \rangle}, \quad (23)$$

where  $\langle \dots \rangle$  denotes an expectation value of the corresponding operator over a quantum state  $|\Psi\rangle$  of the electronic-field Hamiltonian. Using the normalizations  $x = k_f \langle \hat{x} \rangle$ ,  $p = \langle \hat{p} \rangle / \hbar k_f$ , and  $\tau = \Omega_0 t$ , we get from (23)

$$\begin{aligned} \dot{x} &= \alpha p, \\ \dot{p} &= -\langle \Psi(\tau) | \hat{a}^\dagger \hat{\sigma}_- + \hat{a} \hat{\sigma}_+ | \Psi(\tau) \rangle \sin x, \end{aligned} \quad (24)$$

where  $\alpha = \hbar k_f^2 / m_a \Omega_0$  is the normalized recoil frequency which characterizes the average change in kinetic energy of the atom,  $\hbar^2 k_f^2 / 2m_a$ , in the process of

emission and absorption of a photon. After computing the expectation value in (24) with the state vector (9), we obtain our basic Hamilton-Schrödinger equations

$$\begin{aligned} \dot{x} &= \alpha p, \\ \dot{p} &= -\sum_{n=0}^{\infty} \sqrt{n+1} u_n \sin x, \\ \dot{u}_n &= \delta v_n, \\ \dot{v}_n &= -\delta u_n + 2\sqrt{n+1} z_n \cos x, \\ \dot{z}_n &= -2\sqrt{n+1} v_n \cos x, \quad n = 0, 1, 2, \dots \end{aligned} \quad (25)$$

which describe the atom-field quantum-classical hybrid with the quantum degrees of freedom dynamically coupled to the classical degree of freedom. This infinite set of *nonlinear ordinary differential equations* possesses an infinite number of the integrals of motion, the total energy integral

$$W = \frac{\alpha}{2} p^2 - \sum_{n=0}^{\infty} \sqrt{n+1} u_n \cos x - \frac{\delta}{2} \sum_{n=0}^{\infty} z_n, \quad (26)$$

the Bloch-like integral for each  $n$

$$R_n^2 = u_n^2 + v_n^2 + z_n^2, \quad (27)$$

and the global integral

$$\sum_{n=0}^{\infty} R_n = 1. \quad (28)$$

The infinite-dimensional nonlinear dynamical system (25) is a quantum generalization of the five-dimensional semiclassical set of the equations of motion for the same problem that was derived in Refs [21, 22] with a classical field. The later one was shown [21, 22, 26, 27] to be chaotic with positive values of the maximal Lyapunov exponent in some ranges of the system's control parameters. It is rather difficult to compute this quantitative indicator of dynamical chaos with an infinite dimensional set of ODE's. However, we have found another signatures of Hamiltonian chaos with Eqs. (25), the main of which are fractals which will be demonstrated in the next section.

Let us compare the Rabi-oscillation signals with the atom-field quantum-classical hybrid (25) and with the fully quantum Jaynes-Cummings model without recoil (13). In Fig. 2a and b the population inversion  $z$  (see Eq. (15)) for an initially excited atom interacting in resonance with the field that is initially in a coherent state (19) and in a Bose-Einstein state (20), respectively, is shown. This figure should be compared with Fig. 1 where the Rabi oscillations with the Jaynes-Cummings model have been computed for the same initial conditions and the field states with  $\langle n \rangle = 10$  but with a motionless atom. More pronounced collapses and revivals occur with the quantum-classical hybrid as compared with the fully quantum model without recoil. In order to understand peculiarities of

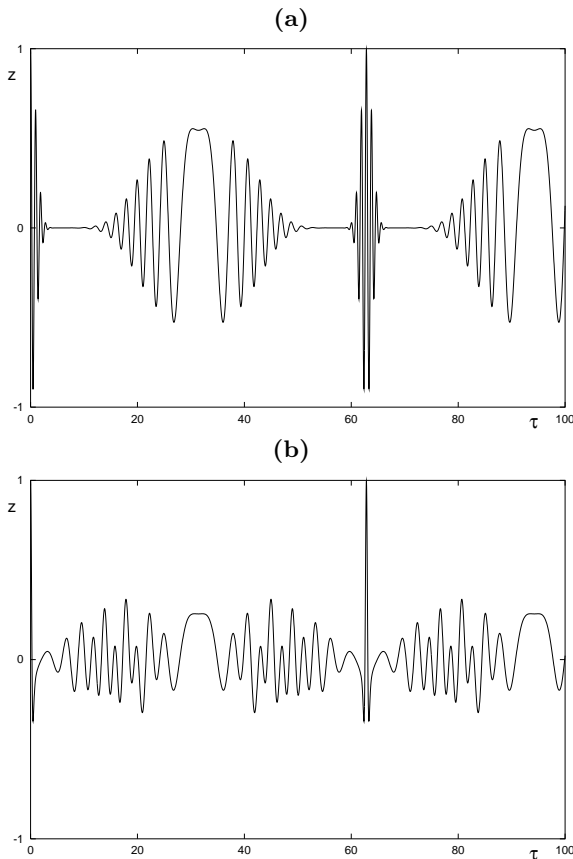


FIG. 2: The same as in FIG. 1 but with the resonant quantum-classical hybrid.

the Rabi oscillations in Fig. 2 look at Fig. 7a demonstrating the scheme of gedanken experiments. An atom starts at  $x = 0$  and moves to the right with the initial momentum  $p_0 = 50$ . It reaches the first node of the standing wave, where the coupling coefficient with the field mode is zero at time moment  $\tau_1 = \pi/2\alpha p_0 \simeq 31.4$  in dimensionless units (we choose  $\alpha = 0.001$  in our computer simulations). For both the field states, one can see the respective slowing down of the Rabi oscillations at the moments of time  $\tau_s = (1+2s)\pi/2\alpha p_0$ , when the atom transverses the  $s$ -th node. The pronounced peaks of revivals of the Rabi oscillations occur at the moments  $\tau_r = r\pi/\alpha p_0$ , when the atom transverses the  $r$ -th antinode of the standing wave where its coupling with the field is maximal.

In spite of a complicated character of the Rabi oscillations, shown in Fig. 2, they are regular because at exact resonance,  $\delta = 0$ , all the values of the real-valued amplitudes  $u_n$  are conserved during the evolution. With initially excited atom we have  $u_n(0) = v_n(0) = 0$  for each  $n$ . It immediately follows from Eqs.(25) that the atom moves with a constant velocity through the cavity. It means that  $x$  is a linear function of time, and the Hamilton-Schrödinger equations(25) reduce to the periodically modulated linear Bloch-like equa-

tions (13) with periodic solutions. The exact solution for the atomic population inversion can be easily found

$$z(\tau) = \sum_{n=0}^{\infty} z_n(0) \cos\left(\frac{2\sqrt{n+1}}{\alpha p_0} \sin \alpha p_0 \tau\right). \quad (29)$$

It is a periodic function (shown in Fig. 2) with the period to be equal to  $\pi/\alpha p_0$  and the maxima at  $\tau_r = r\pi/\alpha p_0$  ( $r = 0, 1, 2, \dots$ ).

Out off resonance,  $\delta \neq 0$ , the quantum-classical hybrid may demonstrate chaos. To diagnose chaos it is instructive to compute the maximal Lyapunov exponent  $\lambda$  whose values depend on initial conditions, on the detuning  $\delta$ , the mean number of photons in the mode, and on the recoil frequency  $\alpha$ . If the quantized field is initially prepared in the Fock state  $|n\rangle$  with exactly  $n$  quanta in the mode, the infinite-dimensional set (25) reduces to 8 equations

$$\begin{aligned} \dot{x} &= \alpha p, \\ \dot{p} &= -(\sqrt{n} u_{n-1} + \sqrt{n+1} u_n) \sin x, \\ \dot{u}_{n-1} &= \delta v_{n-1}, \\ \dot{v}_{n-1} &= -\delta u_{n-1} + 2\sqrt{n} z_{n-1} \cos x, \\ \dot{z}_{n-1} &= -2\sqrt{n} v_{n-1} \cos x, \\ \dot{u}_n &= \delta v_n, \\ \dot{v}_n &= -\delta u_n + 2\sqrt{n+1} z_n \cos x, \\ \dot{z}_n &= -2\sqrt{n+1} v_n \cos x \end{aligned} \quad (30)$$

with initial conditions

$$\begin{aligned} x(0) &= x_0, \quad p(0) = p_0, \\ z_{n-1}(0) &= -|b_n(0)|^2, \quad z_n(0) = |a_n(0)|^2, \\ u_{n-1}(0) &= u_n(0) = v_{n-1}(0) = v_n(0) = 0 \end{aligned} \quad (31)$$

describing the atom-field system initially prepared in a superposition state

$$\begin{aligned} |\Psi(0)\rangle &= a_n(0)|2, n\rangle + b_n(0)|1, n\rangle, \\ |a_n(0)|^2 &+ |b_n(0)|^2 = 1. \end{aligned} \quad (32)$$

The so-called topographic  $\lambda$ -maps, showing by color modulation values of  $\lambda$  in the ranges of values of two control parameters with the third one to be fixed, have been computed with the set (30). In Fig. 3 we show the  $\lambda$ -map with initial zero atomic population,  $a_n(0) = b_n(0) = 1/\sqrt{2}$ ,  $z(0) = z_{n-1}(0) + z_n(0) = 0$ , in the ranges of the detuning  $\delta$  and the recoil frequency  $\alpha$  with the fixed value of the initial number of photons  $n = 10$ . At exact resonance, the set (30) is integrable and  $\lambda = 0$  at  $\delta = 0$ . In the range  $\alpha \sim 10^{-4} \div 10^{-2}$ , that corresponds to realistic values of the recoil frequency, the maximal Lyapunov exponent may be positive and one may expect chaotic atomic motion in the respective ranges of  $\alpha$  and  $\delta$ . Another  $\lambda$ -map with initially excited atom,  $a_n(0) = 1$ ,  $b_n(0) = 0$ ,  $z(0) = 1$ , demonstrates in Fig. 4 the values of  $\lambda$  in dependence on  $\alpha$

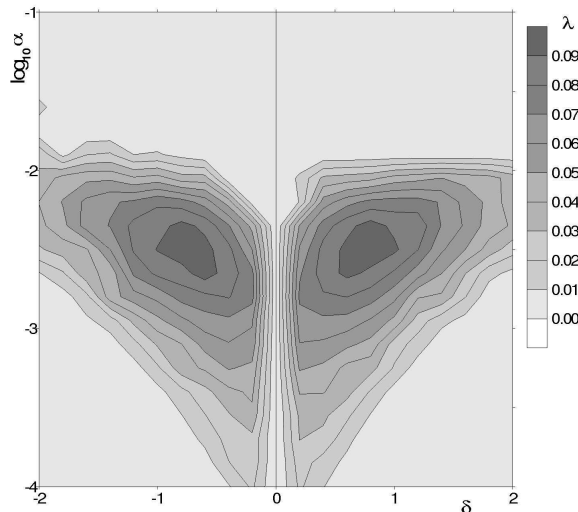


FIG. 3: The maximal Lyapunov exponent  $\lambda$  with the quantum-classical hybrid in the Fock quantized field versus the atom-field detuning  $\delta$  and the logarithm of the dimensionless recoil frequency  $\alpha$ .

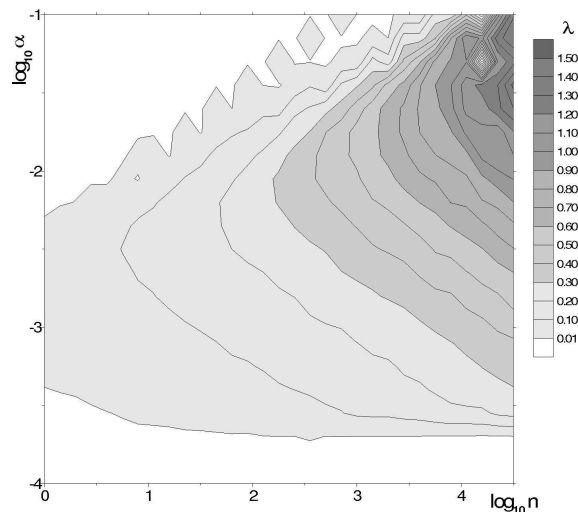


FIG. 4: The double logarithmic plot of  $\lambda$  versus  $\alpha$  and initial number of photons in the Fock field  $n$ .

and  $n$  at  $\delta = 0.5$  in double logarithmic scale. The magnitude of the maximal Lyapunov exponent grows, in average, with increasing the initial number of photons in the cavity mode.

Computing the values of  $\lambda$  is difficult with the cavity field initially prepared in a superposition state (18) (including coherent and Bose-Einstein states) that generates an infinite number of the equations of motion (25). We have found another signatures of chaos. In Fig. 5 an atomic trajectory,  $x(\tau)$ , and oscillations of the atomic momentum,  $p(\tau)$ , are shown to illustrate manifestations of chaos in the set (25) with the initially coherent field and the excited atom

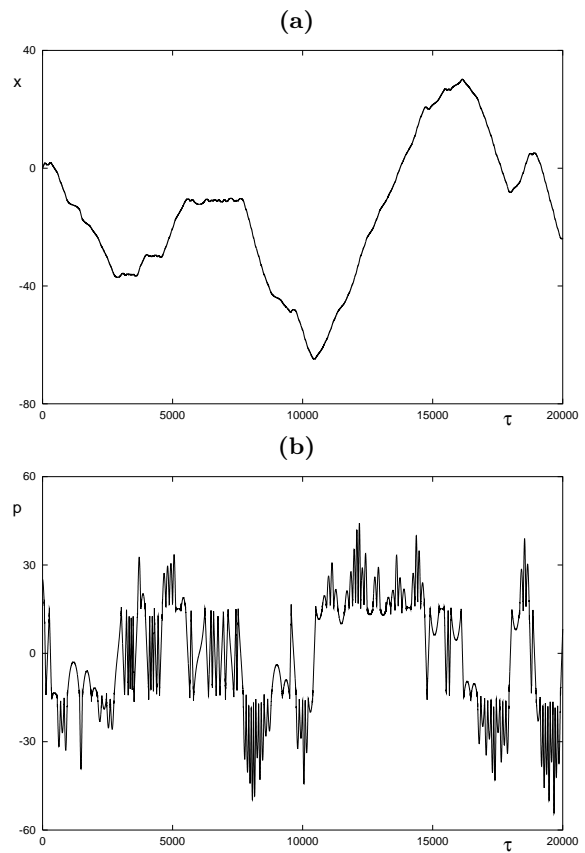


FIG. 5: (a) A chaotic atomic trajectory with an initially coherent field and (b) the respective oscillations of the atomic momentum.

with  $\langle n \rangle = 10$ ,  $\delta = 0.4$ ,  $\alpha = 0.001$ , and  $p_0 = 25$ . A typical weakly chaotic atomic trajectory represents a kind of a random walking with small oscillations of the atom in potential wells, long ballistic flights of the Lévy type with almost constant velocity and erratic turnbacks. Just the presence of Lévy flights fluenses strongly the statistical properties of the system generating power-like statistical laws that have been extensively studied in the semiclassical approximation in Refs.[27, 28]. Fig. 6 presents Poincaré sections of motion in the set (25) with five different values of the initial atomic momentum to be projected on the plane of the atomic external variables  $(x, p)$ . Fig. 6a demonstrates an example of chaotic Poincaré section ( $\delta = 0.1$ ) whereas Fig. 7b presents a regular motion under the same conditions except for the detuning  $\delta = 0.5$ .

A feasible scheme for detecting manifestation of chaos with hot two-level Rydberg atoms moving in a high-Q microwave cavity has been proposed in [26]. The same idea could be realized with cold usual atoms in a high-Q microcavity. Consider a 2D-geometry of a gedanken experiment with a monokinetic atomic beam propagating almost perpendicularly to the cavity axis  $x$ . In a reference frame moving with a constant



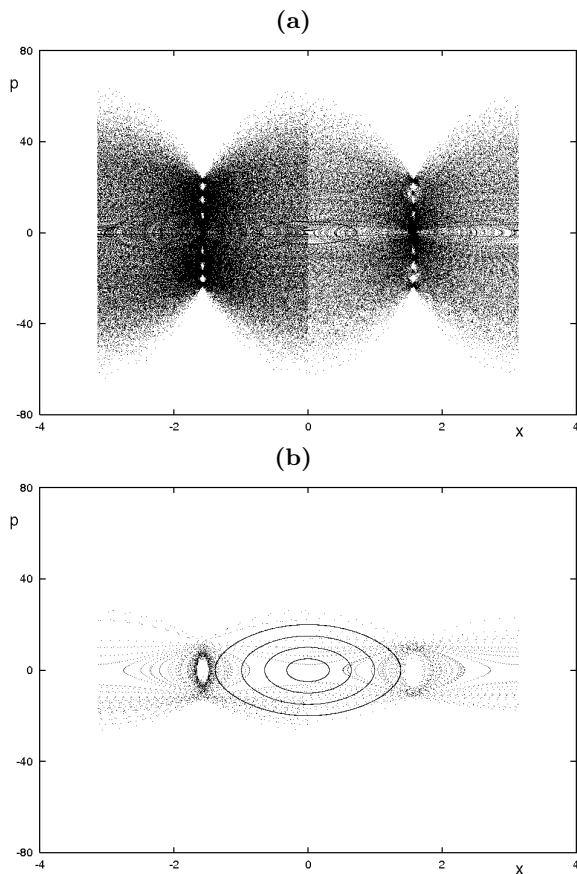


FIG. 6: Projections of the Poincaré sections on the plane of the atomic momentum  $p$  and the position  $x$ . (a) Chaos at  $\delta = 0.1$  and (b) regular motion at  $\delta = 0.5$ .

velocity in the perpendicular direction, there remains only the transverse atomic motion along the axis  $x$ . One measures atomic population inversion after passing the interaction zone. Before injecting atoms in the cavity, it is necessary to prepare all the atoms in the same electronic state, say, in the excited state, with the help of a  $\pi$ -pulse of the laser radiation. It may be done with *only a finite accuracy*, say, equal to  $\Delta z_{\text{in}}$  for the initial population inversion  $z_{\text{in}}$ . The values of the population inversion  $z_{\text{out}}$  are measured with detectors at a fixed time moment. If we would work with the values of the control parameters corresponding to the regular atom-field dynamics, we would expect to have a regular curve  $z_{\text{out}}-z_{\text{in}}$ . In the chaotic regime, the atomic inversion at the output can be predicted (within a certain confidence interval  $\Delta z$ ) for a time not exceeding the so-called predictability horizon

$$\tau_p \simeq \frac{1}{\lambda} \ln \frac{\Delta z}{\Delta z_{\text{in}}}, \quad (33)$$

which depends weakly on  $\Delta z_{\text{in}}$  and  $\Delta z$ . Since the maximal confidence interval lies in the range  $|\Delta z| \leq 1$  and  $\lambda$  may reach the values of the order of 1.5 (see  $\lambda$ -maps), the predictability horizon in accordance with

the formula (33) can be very short: with  $\lambda = 0.5$  the predictability horizon  $\tau_p$  may be of the order of 10 in units reciprocal of the vacuum Rabi frequency  $\Omega_0$  that corresponds to  $t_p \simeq 10^{-7}$  s with the realistic value of  $\Omega_0 \simeq 10^8$  rad·s $^{-1}$ .

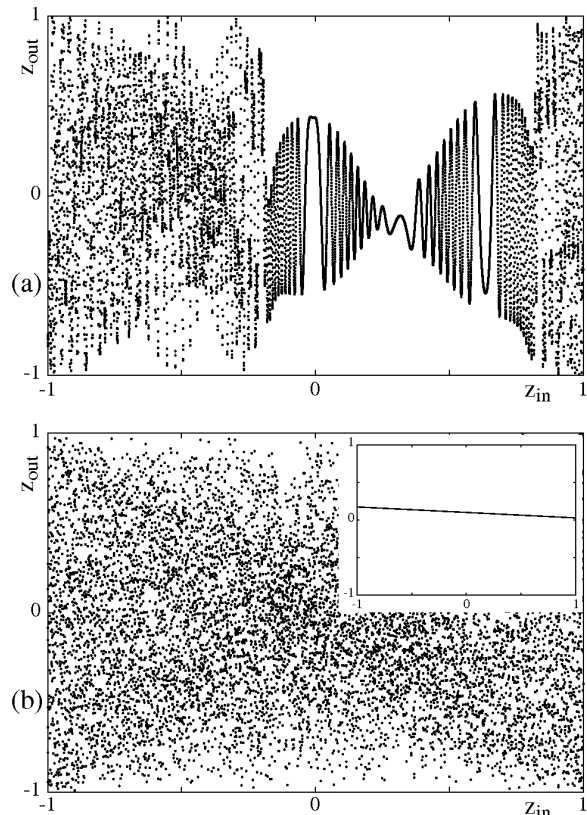


FIG. 7: Dependence of the output values of the atomic population inversion  $z_{\text{out}}$  on its initial values  $z_{\text{in}}$  with  $\delta = 0.4$  (a) at  $\tau = 100$  and (b) at  $\tau = 200$  with the inset showing this dependence at the exact atom-field resonance,  $\delta = 0$ .

In the regular regime, the inevitable errors in preparing  $\Delta z_{\text{in}}$  produce the output errors  $\Delta z_{\text{out}}$  of the same order. In the chaotic regime, the initial uncertainty increases exponentially resulting in a complete uncertainty of the detected population inversion in a reasonable time. It is demonstrated in Fig. 7, where we plot the dependence of the values of  $z(\tau) = z_{\text{out}}$  at  $\tau = 100$  (Fig. 7a) and  $\tau = 200$  (Fig. 7b) on the values of  $z(0) = z_{\text{in}}$  in the chaotic regime with an initially Fock field at  $\delta = 0.4$  and  $\lambda \simeq 0.05$ . Simulation shows that an initial error  $\Delta z_{\text{in}} = 10^{-4}$  in preparing the atomic electronic state leads to complete uncertainty  $\Delta z_{\text{out}} \simeq 2$  in a rather short time. To see the difference, it is desirable to carry out a control experiment at the exact resonance ( $\delta = 0$ ) when the atomic motion is fully regular with any initial values. The dependence  $z_{\text{out}}-z_{\text{in}}$  with  $\delta = 0$  is demonstrated in the inset in Fig. 7b with all the other control parameters and initial values being the same.

## V. ATOMIC DYNAMICAL FRACTALS

In this section, we treat the atom-photon interaction in a high- $Q$  cavity as a chaotic scattering problem. Let us consider the scheme of scattering of atoms by

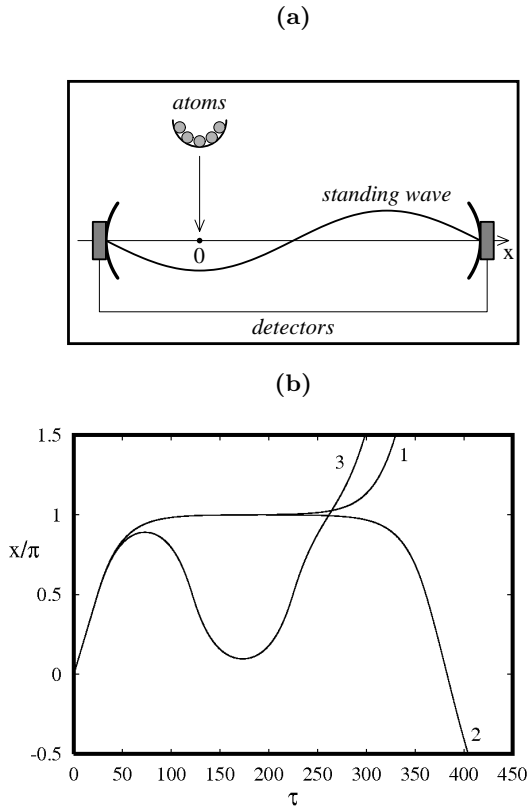


FIG. 8: (a) Schematic diagram showing scattering of atoms at the standing wave and (b) sample atomic trajectories.

the standing wave shown in Fig. 8a. Atoms, one by one, are placed at the point  $x = 0$  with different initial values of the momentum  $p_0$  along the cavity axis. For simplicity, we suppose that they have no momentum in the other directions (1D-geometry). We compute the time the atoms need to reach one of the detectors placed at the cavity mirrors. The dependence of this exit time  $T$  on the initial atomic momentum  $p_0$  is studied under the other initial conditions and parameters being the same. To avoid complications that are not essential to the main theme of this section, we consider the cavity with only two standing-wave lengths.

### A. Fock fractal

In this subsection the field is supposed to be initially prepared in a Fock state. Before injecting into a cavity, atoms are supposed to be prepared in the superposition state with  $u_{n-1}(0) = u_n(0) = v_{n-1}(0) = v_n(0) =$

$0$ ,  $z_{n-1}(0) = -1/2$ ,  $z_n(0) = 1/2$ , i. e. in the state with zero population inversion  $z(0) = z_{n-1}(0) + z_n(0) = 0$ .

At exact resonance ( $\delta = 0$ ) with  $u_{n-1}(\tau) = u_n(\tau) = 0$ , the optical potential  $U = (\sqrt{n}u_{n-1} + \sqrt{n+1}u_n) \cos x - \delta(z_{n-1} + z_n)/2$  is equal to zero, and the analytical expression for the dependence in question can be easily found to be the following:

$$\begin{aligned} T(\delta = 0) &= 3\pi/2\alpha p_0 \text{ if } p_0 > 0, \\ T(\delta = 0) &= \pi/2\alpha p_0 \text{ if } p_0 < 0. \end{aligned} \quad (34)$$

Atoms simply fly through the cavity in one direction with their initial constant velocity and are registered by one of the detectors. Out of resonance ( $\delta \neq 0$ ), the atomic motion has been numerically found in preceding section to be chaotic with positive values of the maximal Lyapunov exponent in the following ranges of the values of the control parameters: the detuning  $|\delta| \lesssim 2$  and the recoil frequency  $\alpha \simeq 10^{-4} \div 10^{-2}$ . Fig. 9 shows the function  $T(p_0)$  with the normalized detuning  $\delta = 0.4$ , the recoil frequency  $\alpha = 10^{-3}$ , and the initial number of cavity photons  $n = 10$ . The exit-time function demonstrates an intermittency of smooth curves and complicated structures that cannot be resolved in principle, no matter how large the magnification factor. Fig. 9b shows magnification of the function for the small interval  $64.1 \leq p_0 \leq 64.6$ . Further magnification in the range  $64.2743 \leq p_0 \leq 64.2754$  shown in Fig. 9c reveals a beautiful self-similar structure. Some structures in Fig. 9a that look like fractal are not, in fact, unresolvable and self-similar. Magnification of the structure in the range  $73.2 \leq p_0 \leq 73.8$  demonstrates quite a smooth function without unresolvable substructures and with only two singular points on the borders of the respective momentum interval. Beating in all the structures of the atomic fractal in Fig. 9 should be attributed to the structure of the Hamilton-Schrödinger equations (30) which describe two atom-field oscillators with slightly different frequencies.

The exit time  $T$ , corresponding to both smooth and unresolved  $p_0$  intervals, increases in average with increasing the magnification factor. It follows that there exist atoms never reaching the detectors in spite of the fact that they have no obvious energy restrictions to leave the cavity. Tiny interplay between chaotic external and internal dynamics prevents these atoms from leaving the cavity. The similar phenomenon in Hamiltonian systems is known as *dynamical trapping* [29]. Different kinds of atomic trajectories, which are computed with the system (30), are shown in Fig. 8b. A trajectory with the number  $m$  transverses the central node of the standing-wave, before being detected,  $m$  times and is called  $m$ -th trajectory. There are also special separatrix-like  $mS$ -trajectories following which atoms in infinite time reach the stationary points  $x_s = \pm\pi s$  ( $s = 0, 1, 2, \dots$ ),  $p_s = 0$ , transversing  $m$  times the central node. These points are the anti-nodes of the standing wave where the force acting on atoms is zero. A detuned atom can asymptotically

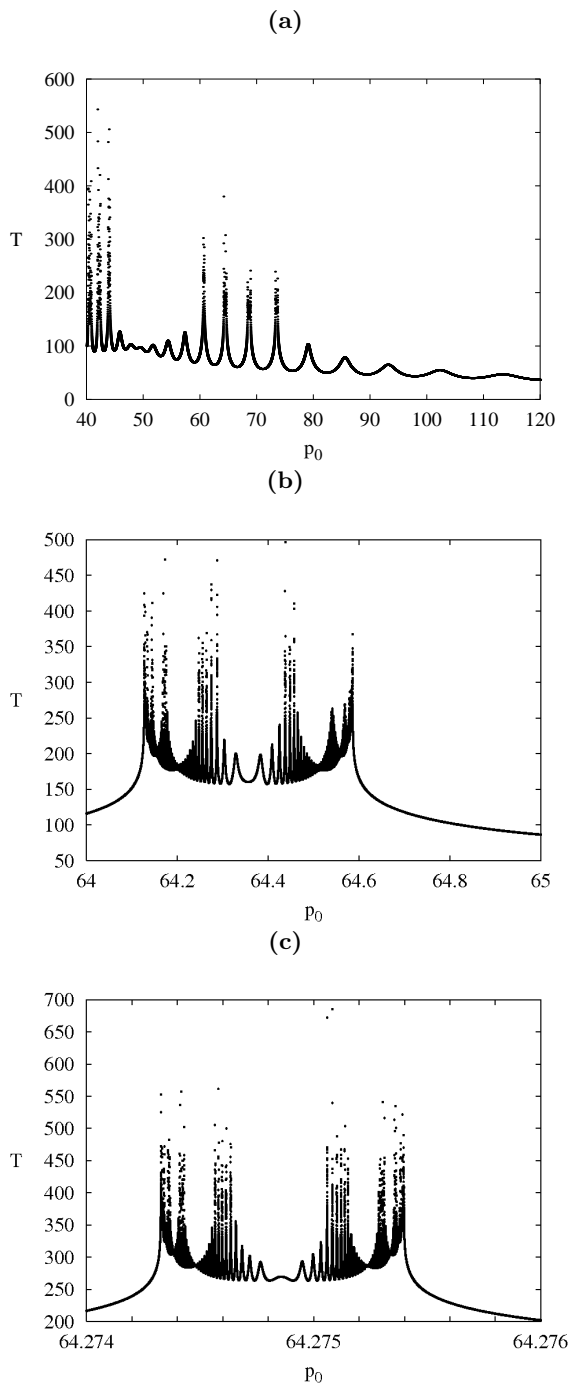


FIG. 9: Fock atomic fractal with different resolutions.

reach one of the stationary points after transversing the central node  $m$  times. The trajectory with number 1, showing in Fig. 8b, is close to a separatrix-like  $1S$ -trajectory. The smooth  $p_0$  intervals in the first-order structure in Fig. 9a correspond to atoms transversing once the central node and reaching the right detector. The unresolved singular points in the first-order structure with  $T = \infty$  at the border between the smooth and unresolved  $p_0$  intervals are generated by the  $1S$ -trajectories. Analogously, the smooth  $p_0$  intervals in

the second-order structure in Fig. 9b correspond to the 2-nd order trajectories with singular points between them corresponding to the  $2S$ -trajectories and so on.

There are two different mechanisms of generation of infinite exit times, namely, dynamical trapping with infinite oscillations ( $m = \infty$ ) in a cavity and the separatrix-like motion ( $m \neq \infty$ ). The set of all initial momenta generating the separatrix-like trajectories is a countable fractal. Each point in the set can be specified as a vector in a Hilbert space with  $m$  integer nonzero components. One is able to prescribe to any unresolved interval of a  $m$ -th order structure a set with  $m$  integers, where the first integer is a number of a second-order structure to which trajectory under consideration belongs in the first-order structure, the second integer is a number of a third-order structure in the second-order structure mentioned above, and so on. Such a number set is analogous to a directory tree address: “<a subdirectory of the root directory>/<a subdirectory of the 2-nd level>/<a subdirectory of the 3-rd level>/...”. Unlike the separatrix fractal, the set of all initial atomic momenta leading to dynamically trapped atoms with  $m = \infty$  seems to be uncountable.

Nonlinear fractal dynamics implies specific statistical properties of chaotic motion in Hamiltonian systems (for a review see [29]). Even a finite-dimensional atom-field system’s phase space has a complicated topology whose simplified image is given by projections of Poincaré sections and fractal scattering functions. Tiny interplay between all the degrees of freedom is responsible for dynamical trapping of atoms even in a very short microcavity and for anomalous statistical properties of the fundamental atom-photon interaction. The probability distribution of exit times  $P(T)$  for  $2 \cdot 10^5$  events with initial atomic momenta in the range  $8 \leq p_0 \leq 40$  is shown in Fig. 10a in double logarithmic scale. It is close to a Poissonian distribution with comparatively short exit times up to  $T \simeq 300$  and demonstrates an algebraic decay with the characteristic exponent  $\gamma \simeq -3.72$  at its tail ( $\leq 300T \leq 4000$ ). In the range of initial atomic momenta  $40 \leq p_0 \leq 41$ , the respective PDF for  $1.5 \cdot 10^6$  events is computed under the same other conditions to be a Poissonian-like.

## B. Coherent fractal

Following to the scheme in Fig. 8a, let us consider in this section scattering of atoms by the standing wave field initially prepared in the coherent state (19). Before injecting into a cavity, atoms supposed to be prepared in the excited state  $|2\rangle$  with  $z(0) = 1$ . In this case the initial conditions are

$$\begin{aligned} u_n(0) &= v_n(0) = 0, \quad \forall n, \\ z_n(0) &= e^{-\langle n \rangle} \frac{\langle n \rangle^n}{n!}. \end{aligned} \quad (35)$$

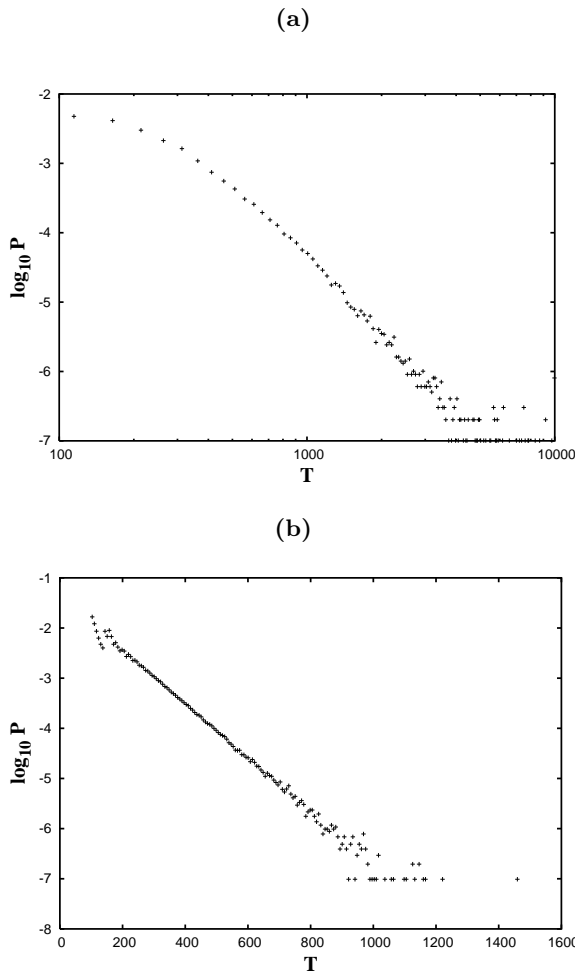


FIG. 10: Exit-time distributions in the Fock field: (a) an algebraic decay in the range of initial atomic momenta  $8 \leq p_0 \leq 40$  and an exponential decay in the range of initial atomic momenta  $40 \leq p_0 \leq 41$ .

Fig. 11 demonstrates the respective exit-time function  $T(p_0)$  with  $\delta = 0.1$ ,  $\alpha = 0.001$ , and  $\langle n \rangle = 10$ . A coherent state is not a sharply defined state, as a Fock one, but a superposition of an infinite number of Fock states. We used a truncated basis of 1000 Fock states for the cavity mode in our simulation. Resolution of one of the unresolved structures in Fig. 11a is shown in Fig. 11b. It resembles the respective fragment of the Fock fractal in Fig. 9b. Further magnification of the function in Fig. 11b, which is shown in Fig. 11c, reveals again a self-similar structure with smooth and singular zones.

We collect an exit time statistics with  $6 \cdot 10^5$  events by counting atoms with initial momenta in the range  $9 \leq p_0 \leq 30$  reaching the detectors. The plot of the respective histogram of exit times, shown in Fig. 12, demonstrates a few local maxima. The corresponding times of exit of atoms can be approximately estimated with the help of the formula (35) for resonant atoms. The first maximum around  $T \simeq 150 \div 160$  corresponds,

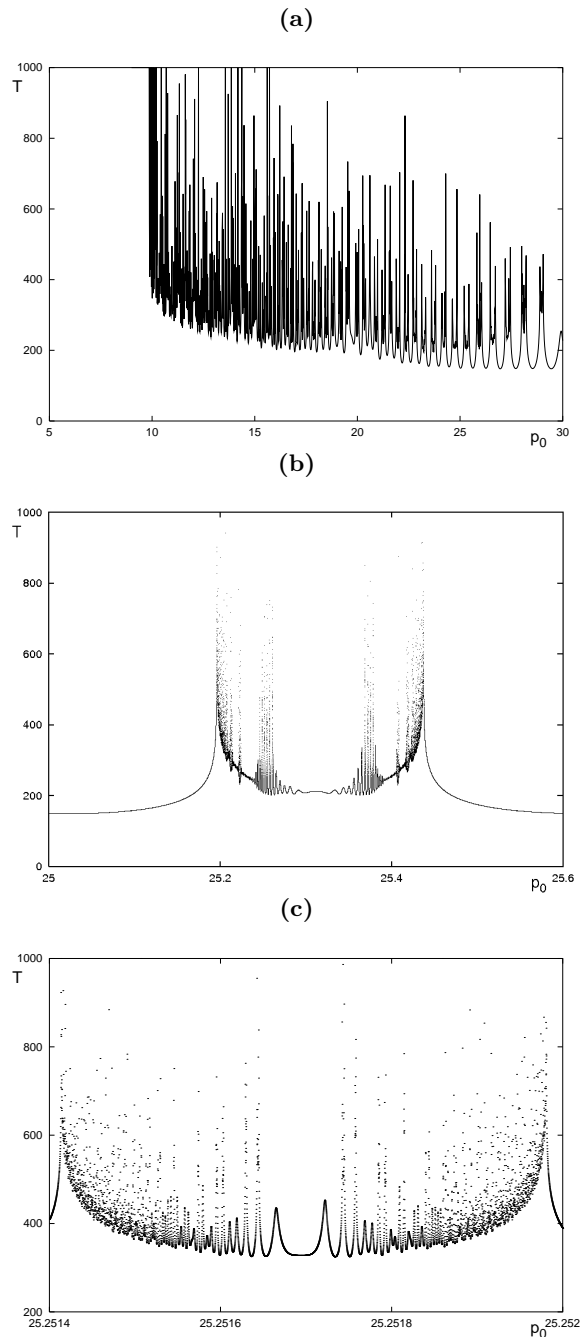


FIG. 11: Coherent atomic fractal with different resolutions.

mainly, to atoms which, being initially directed to the right with comparatively low momenta  $p_0 \simeq 10$ , turn back before reaching the central node and are registered by the left detector. It follows from (35) that for such atoms  $T_1 \simeq \pi/2\alpha p_0 \simeq 157$  at  $\alpha p_0 = 0.01$ . However, the atoms, to be injected initially with the momentum  $p_0 \simeq 20 \div 25$  and registered by the right detector, may contribute to the first maximum as well because, after transversing the central node, they can be accelerated and gain the values of the momentum  $p$

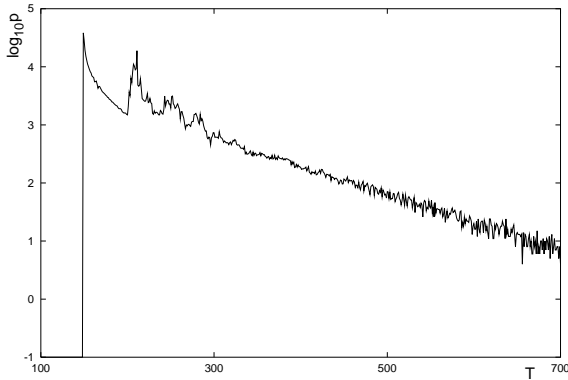


FIG. 12: Exit-time distribution in the coherent field.

up to 50. The second local maximum around  $T \simeq 200$  corresponds, mainly, to atoms with  $p_0 \simeq 20 \div 30$  which transverse the central node and are registered by the right detector for the time  $T_2 \sim 3\pi/2\alpha p_0$ . The other local maxima of the PDF are not so pronounced as the first ones, they are formed by the atoms transverse the central node a few times. The PDF in Fig. 12 demonstrates an exponential decay at the tail up to the exit times  $T = 700$ .

### C. Bose-Einstein fractal

In conclusion of this section we present in Fig. 13 the fractal computed with the field initially prepared in a Bose-Einstein state (20) and atoms supposed to be prepared in the excited state  $|2\rangle$  with  $z(0) = 1$ . The initial conditions are

$$\begin{aligned} u_n(0) &= v_n(0) = 0, \quad \forall n, \\ z_n(0) &= \frac{\langle n \rangle^n}{(1 + \langle n \rangle)^{n+1}}. \end{aligned} \quad (36)$$

The values of the control parameters are the same as for the coherent fractal. Fig. 13 demonstrates again a self-similar structure of the exit-time distribution. We want to stress that the Hamilton-Schrödinger sets of equations generating the Fock and the other fractals differ strongly in the number of equations. Nevertheless, the respective  $T(p_0)$  functions are rather similar in their main features. The atomic fractals we have found are generated by dynamical chaos in the atom-photon interaction but not by noise.

## VI. CONCLUSION

We have studied in the strong-coupling regime the fundamental interaction between a two-level atom with recoil and a quantized radiation field in a single-mode cavity in the mixed quantum-classical formalism modelling quantum evolution of the electronic-field

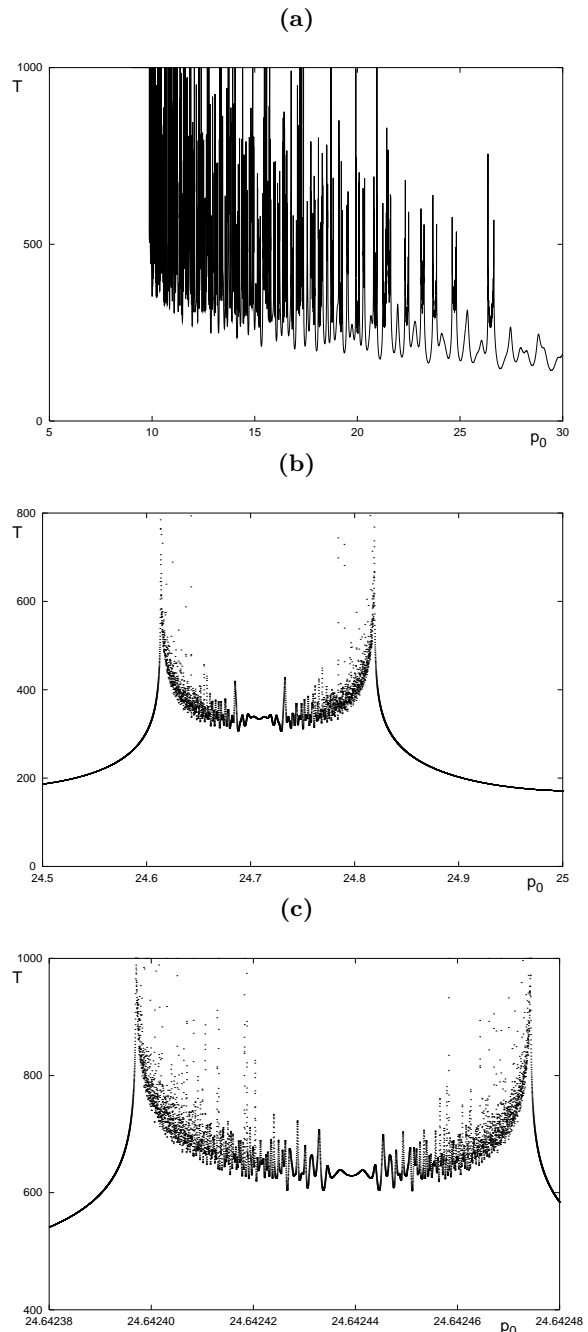


FIG. 13: Bose-Einstein atomic fractal with different resolutions.

purely quantum system to be disturbed by translational atomic motion. We have managed to derive an infinite set of the Hamilton-Schrödinger nonlinear ODE's for real valued electronic-field probability amplitudes and expectation values of the atomic center-of-mass position and momentum. These equations of motion are able to demonstrate known features of the atom-field quantum evolution in the strong-coupling limit such as collapses and revivals of the atomic population inversion modulated by atomic motion through

the nodes and antinodes of the standing wave. We have shown that even in the absence of any other interaction with environment the Hamilton-Schrödinger dynamical system provides the emergence of classical Hamiltonian dynamical chaos from cavity quantum electrodynamics.

We have investigated the atom-photon nonlinear dynamics with Fock, coherent and Bose-Einstein quantum states of the initial cavity field. Positive values of the maximal Lyapunov exponent  $\lambda$  have been found with reasonable values of the control parameters, the detuning of the atom-field resonance,  $\delta$ , the atomic recoil frequency,  $\alpha$ , and the initial mean number of photons. Exponential sensitivity to initial conditions may manifest itself in the chaotic dependence of the output values of the atomic population inversion on its input values that may, in principle, be measured in real experiments. New manifestations of Hamiltonian chaos in the atom-photon interaction, we have found numerically in the dependence of the atomic exit times on the initial momentum, are atomic fractals. They were classified by the names of the respective quantum field states, i.e., the Fock, coherent and

Bose-Einstein fractals. We have found anomalous statistical properties of the chaotic atom-photon interaction: Lévy atomic flights through a cavity and a power law at the tail of the exit-time distribution function in the Fock field. Power-law tails should appear (at least, in some ranges of the control parameters) in the PDF's with coherent and Bose-Einstein fields, as well, but their detection would require a longer computation time than we have used.

### Acknowledgments

I am grateful to Leonid Kon'kov and Michael Uleysky for preparing the figures. This work was supported by the Russian Foundation for Basic Research under Grant No. 02-02-17796, by the Program "Mathematical Methods in Nonlinear Dynamics" of the Russian Academy of Sciences, and by the Program for Basic Research of the Far Eastern Division of the Russian Academy of Sciences.

- 
- [1] B.V. Chirikov, Phys. Rep. 52 (1979) 263.
  - [2] G.M. Zaslavsky, Phys. Rep. 80 (1981) 157.
  - [3] F. Haake, *Quantum Signatures of Chaos*, Springer, Berlin (1991).
  - [4] M.C. Gutzwiller, *Chaos in Classical and Quantum Mechanics*, Springer, New York (1990).
  - [5] *Cavity Quantum Electrodynamics*, ed. by P.R. Berman, Academic Press, New York (1994).
  - [6] H. Walther, Phys. Rep. 219 (1992) 263.
  - [7] J. M. Raimond, M. Brune, S. Haroche, Rev. Mod. Phys. 73 (2001) 565.
  - [8] W. Vogel, D.-G. Welsch, S. Wallentowitz, *Quantum Optics: An Introduction*, Wiley-VCH, Berlin (2001).
  - [9] J.R. Ackerhalt, P.W. Milonni, M.-L. Shih, Phys. Rep. 128 (1985) 205.
  - [10] R.G. Harrison, Contemp. Phys. 29 (1988) 341.
  - [11] Ya.I. Khanin, *Foundations of Laser Dynamics*, Nauka, Moscow (1999) [in Russian].
  - [12] H. Haken, Phys. Lett. A 53 (1975) 77.
  - [13] P.I. Belobrov, G.M. Zaslavskii, G.Kh. Tartakovskii, Zh. Eksp. Teor. Fiz. 71 (1976) 1799 [Sov. Phys. JETP 44 (1976) 945].
  - [14] R.M. Dicke, Phys. Rev. 93 (1954) 493.
  - [15] S.V. Prants, L.E. Kon'kov, Pis'ma Zh. Eksp. Teor. Fiz. 65 (1997) 801 [JETP Lett. 65 (1997) 833].
  - [16] S.V. Prants, L.E. Kon'kov, Phys. Lett. A 225 (1997) 33.
  - [17] S.V. Prants, L.E. Kon'kov, Zh. Eksp. Teor. Fiz. 115 (1999) 740 [JETP 88 (1999) 406].
  - [18] S.V. Prants, L.E. Kon'kov, I.L. Kirilyuk, Phys. Rev. E 60 (1999) 335.
  - [19] S.V. Prants, L.E. Kon'kov, Phys. Rev. E 61 (2000) 3632.
  - [20] V.I. Ioussoupov, L.E. Kon'kov, S.V. Prants, Physica D 155 (2001) 311.
  - [21] S.V. Prants, L.E. Kon'kov, Pis'ma Zh. Eksp. Teor. Fiz. 73 (2001) 200 [JETP Lett. 73 (2001) 180].
  - [22] S.V. Prants, V.Yu. Sirotkin, Phys. Rev. A 64 (2001) 033412.
  - [23] E.T. Jaynes, F.W. Cummings, Proc. IEEE 51 (1963) 89.
  - [24] J.M. Raimond, S. Haroche, in: *Confined Electrons and Photons*, ed. by E. Burstein and C. Weisbuch, Plenum Press, New York, 1995.
  - [25] G. Rempe, H. Walther, N. Klein, Phys. Rev. Lett. 58 (1987) 353.
  - [26] S.V. Prants, Pis'ma Zh. Eksp. Teor. Fiz. 75 (2002) 777 [JETP Letters 75 (2002) 651].
  - [27] S.V. Prants, M. Edelman, G.M. Zaslavsky, Phys. Rev. E 66 (2002) 046222.
  - [28] V.Yu. Argonov, S.V. Prants, Zh. Eksp. Teor. Fiz. 123 (2003) 946. [JETP 96 (2003) 832].
  - [29] G.M. Zaslavsky, *Physics of Chaos in Hamiltonian Systems*, Academic Press, Oxford, 1998.